Bionic-inspired Construction of Zn(4,4'-dipy)(OAc)2/Bacterial Cellulose Composite Membrane for Efficient Separation Synergistically Adsorption of Nitrogen and Phosphorus

Xudong Zheng (zheng@cczu.edu.cn)
Changzhou University
Wen Sun
Changzhou University
Ning Wei
Changzhou University
Tingting Bian
Changzhou University
Yi Zhang
Changzhou University
Lingli Li
Changzhou University
Yuzhe Zhang
Changzhou University
Zhongyu Li
Changzhou University
Hongxiang Ou
Changzhou University

Research Article

Keywords: Phosphorus, Ammonia nitrogen, Adsorption, Bacterial cellulose, Membrane, Tannic acid

Posted Date: March 16th, 2021

DOI: https://doi.org/10.21203/rs.3.rs-295433/v1

Bionic-inspired Construction of Zn(4,4'-dipy)$(OAc)_2$/Bacterial Cellulose Composite Membrane for Efficient Separation Synergistically Adsorption of Nitrogen and Phosphorus

Xudong Zheng[a]*, Wen Sun[a], Ning Wei[a], Tingting Bian[a], Yi Zhang[a], Lingli Li[a], Yuzhe Zhang[a], Zhongyu Li[a, b, c], Hongxiang Ou[a]*

[a] School of Environmental & Safety Engineering, Changzhou University, Changzhou 213164, PR China

[b] Jiangsu Key Laboratory of Advanced Catalytic Materials and Technology, School of Petrochemical Engineering, Changzhou University, Changzhou 213164, PR China

[c] Advanced Catalysis and Green Manufacturing Collaborative Innovation Center, Changzhou University, Changzhou 213164, PR China

* Corresponding author.

Mail address: zheng@cczu.edu.cn

Postal address: Mingxing Building, Science and Education City, Wujin District, Changzhou, Jiangsu, China

Abstract

Phosphorus and nitrogen flow to water leads to eutrophication and depletion of reserves. Bionic-inspired tannin modification is proposed for preparing a tannin-modified La-Zn(4,4'-dipy)$(OAc)_2$/bacterial cellulose composite membrane for simultaneous adsorption of total phosphorus and ammonia nitrogen in water. Its physical and chemical properties were characterized by XRD, SEM, FT-IR, TGA and other characterization. La-Zn(4,4'-dipy)$(OAc)_2$ nanomaterial achieved effective adhesion on the tannin-modified bacterial cellulose membrane. Adsorption experiments showed that the composite membrane can both adsorb total phosphorus and ammonia nitrogen, and adsorption capacity of ammonia nitrogen is better than that of total phosphorus. The maximum adsorption capacities of ammonia nitrogen and total phosphorus are 482.35 mg/g and 374.71 mg/g. In the binary solution, the adsorption capacity of the composite membrane to ammonia nitrogen and total phosphorus decreased, but the adsorption capacity to phosphorus decreased slightly. Results of adsorption experiments showed that the adsorption process of nitrogen and phosphorus by the composite membrane belongs to single-layer adsorption, and the calculation results of the kinetic equation are in accordance with the quasi-second-order, and the adsorption equilibrium of the composite membrane was reached within 360 min. In short, the composite membrane has a better adsorption and separation effect both on ammonia nitrogen and total phosphorus.

Keywords

Phosphorus; Ammonia nitrogen; Adsorption; Bacterial cellulose; Membrane; Tannic acid

1. Introduction

Water eutrophication, driven by rapid population growth has become a threat to human existence and thus regarded as one of most common environmental problems worldwide.(Copetti et al. 2016; Schindler 2012) Especially, China have suffered from eutrophication for decades.(Shi et al. 2019; Yan et al. 2019; Zhang et al. 2020a) Diffuse nitrogen and phosphorus pollutions are now regard as the main drivers of water eutrophication.(Li et al. 2019a; Taipale et al. 2019) So, reduce the content of total phosphorus (TP) and ammonia nitrogen in water is an effective way to control eutrophication. At present, there are mainly three practical repair methods: engineering repair, chemical repair, and biological repair. Engineering repair removes nutrients from the surface sediments in water by hydraulic or mechanical means.(Bormans et al. 2016) The effect of engineering repair is remarkable. However, harmful ingredients such as large amounts of nutrients and heavy metals may return to the water body and cause secondary pollution. The water diversion will reduce the environmental pressure that restricts the growth and reproduction of algae because of the dilution effect. So, when water diversion is taken, the algae will show a momentum of increasing growth. The biological repair is a long-term and effective measure to eliminate the endogenous pollution in the water body.(Zhang et al. 2019) The biological method has the advantages of low cost, sustainability, simple operation, convenient management, and significant purification effect. But long-time process makes it unusable for the treatment of sudden and acute water pollution. For soluble nutrients, chemical repair is

often the simplest and fastest method. The traditional chemical repair adopts methods such as adding chemicals into the water to form an insoluble precipitate. However, the use of agents will harm non-target organisms in water seriously and easy to cause secondary water pollution. So, green chemical treatments have always been a hot topic in water research.(Qiu et al. 2019)

Membrane adsorption is a greener and simpler than traditional chemical treatment. There are many selective adsorption sites on the surface of the membrane through chemical modification or material combination. When the continuous medium flows through membranes, membranes can selectively adsorb and separate specific pollutants.(Zhao et al. 2017; Zhu et al. 2017) Selective groups are firmly fixed on the surface of membrane materials through chemical modification so that the possibility of secondary pollution is very low. In addition, the macro size of the membrane materials makes membranes are very conducive to the treatment and separation process after adsorption compared with current nano-adsorption materials.(Wang et al. 2020) So, Membrane adsorption process has a huge application prospect in the field of environmental governance. Chemical modification requires strict reaction conditions and cumbersome steps, resulting in a higher composition of modified membrane materials. Inspired by the natural adhesion of biological mussels, we use tannic acid (TA) to construct a biomimetic membrane adsorption material.

TA is a typical natural polyphenol compound with a large number of hydroxyl groups, which can interact with the biopolymer (for example, some proteins, digestive

85 enzymes, carbohydrates and minerals, etc.) to provide more chemical properties for the
86 tannic acid. TA can adhere to a variety of substrates, thanks to its surface catechol and
87 catechol groups and a large number of hydroxyl groups. (Li et al. 2020) Ejima et al
88 reported a green, simple and rapid coating method, in which TA and Fe^{3+} were used to
89 synthesize metal organic coordination compounds on various substrates to assemble
90 functional organic membranes step by step.(Ejima et al. 2013)

91 Previously mentioned, controlling TP and ammonia nitrogen in water is an
92 effective way to govern eutrophication. As far as we know, there have been few reports
93 on the selective control of these two substances simultaneously. We use bacterial
94 cellulose (BC) as the membrane substrate due to its excellent pore structure and low
95 cost. But adsorption capacity of bacterial cellulose membrane for TP and ammonia
96 nitrogen is poor and non-selective. TA can be used as an excellent modifier and bond
97 bridge connector. different materials can be simply bonded to the membrane surface to
98 achieve selective adsorption of different substances. Moreover, TA can exhibit strong
99 interactions through multiple hydrogen bonds and hydrophobic interactions.(Shi et al.
100 2020) TA modified membrane materials can not only provide excellent adsorption sites,
101 but also provide better secondary reaction platform to optimize adsorption. So, we use
102 TA modified bacterial cellulose to construct efficient membrane adsorbent materials.
103 Through biomimetic bonding, lanthanum-modified metal organic frame (La-Zn(4,4'-
104 dipy)$(OAc)_2$) is bonded to the membrane surface to construct a membrane adsorption
105 material with selective double adsorption for phosphorus and ammonia nitrogen.

2. Experimental

2.1 Instrumentations and materials

The surface morphology was characterized by Scanning electron microscope (SEM, SUPRA 55, Germany). The Fourier transform infrared (FT-IR) spectrum was studied by IS50 spectrophotometer (United States). The spectral recording range was 4000-500 cm^{-1}. Thermogravimetric analysis (TGA) was performed on the material using a thermogravimetric analyzer (Q600-TGA/DSC, USA) under N_2 atmosphere. The X-ray diffraction (XRD) pattern is collected on Rigaku D/max 2500VL diffractometer (Japan) in a Bragg-Brentano configuration with an Angle 2θ of 5 to 80° to show the change in the crystal structure of the films.

$Zn(OCOCH_3)_2 \cdot 2H_2O$, 4,4'-bipyridine, $La(NO_3)_3$ and acetonitrile were purchased from Aladdin (Shanghai, China), tannic acid, ammonia chloride, potassium dihydrogen phosphate and methanol were purchased from Sinopharm Group Chemical Reagent Co., Ltd. (Shanghai, China)

2.2 Preparation of La-Zn (4,4'-dipy)$(OAc)_2$

A metal organic framework material with Zn^{2+} as the metal ion junction and 4,4'-bipyridine as the organic ligand linking bridge was prepared, in which Zn^{2+} was provided by $Zn(OCOCH_3)_2 \cdot 2H_2O$ reagent. The $Zn(OCOCH_3)_2 \cdot 2H_2O$ and 4,4'-bipyridine with a millimolar ratio of 2:1 were placed in a mixed solution of methanol/water, in which the volumes of methanol and distilled water were both 5 mL, and stirred for 15 min to make the mixture uniform. The solution was sealed in a teflon

reactor, and the yellow needle-like crystals were obtained after reacting at 60 ºC for 24 hours. After washing with methanol and drying in a vacuum oven, and noted as Zn (4,4'-dipy)$(OAc)_2$. Weighing 50 mg of Zn (4,4'-dipy)$(OAc)_2$ and 25 mg of $La(NO_3)_3$, mixed with 10 mL of acetonitrile, and refluxed at 80 ºC for 2 hours. Then it was centrifuged for 15 min, washed with methanol multiple times, and dried at 100 ºC for 1 hour.

2.3 Preparation of tannic acid modified BC membrane

BC membrane was immersed in a 5 mg/mL of tannic acid solution, and replace the tannic acid solution every 12 hours for a total of 6 times. The tannic acid modified BC membrane was washed with deionized water and ethanol and dried in vacuum at 60 ºC for 12 hours.

2.4 Preparation of tannic acid modified La-Zn(4,4'-dipy)$(OAc)_2$/BC composite membrane

According to the above method, the tannic acid modified La-Zn(4,4'-dipy)$(OAc)_2$/BC composite membrane was prepared. First, the BC membrane was modified with tannic acid, then the $Zn(OCOCH_3)_2 \cdot 2H_2O$ and 4,4'-bipyridine were weighed, and mixed with methanol and water, and then the modified tannic acid BC membrane was placed in it and reacted together in a teflon reactor for 24 hours at room temperature. After washing and drying the obtained composite membrane with methanol for several times, the composite membrane was refluxed at 80 ºC for 2 hours in the mixed solution of $La(NO_3)_3$ and acetonitrile. After washing with methanol for

148 several times, and dried. The preparation process is shown in Figure 1.

149 2.5 Effect of pH on adsorption

150 In this experiment, a binary mixed solution with NH_4^+-N and TP concentrations of
151 100 mg/L were prepared using NH_4Cl and KH_2PO_4. H_2SO_4 as an acid regulator,
152 adjusting the pH of the mixed solution to 2.0, 4.0 and 6.0, and NaOH was used to adjust
153 the pH of solution to 7.0, 8.0, 10.0 and 12.0, take 10 mL of pH-adjusted binary solution,
154 add 10 mg of tannin-modified La-Zn(4,4'-dipy)$(OAc)_2$/BC composite membrane, and
155 shake at 25 ºC for 24 hour. The concentration of ammonia nitrogen and total phosphorus
156 in water were measured by Nessler reagent colorimetry and ammonium molybdate
157 spectrophotometry, respectively. Calculate the adsorption capacity (Q_e) by formula (1):

158 $$Q_e = \frac{(C_0 - C_e) \times V}{W} \quad (1)$$

159 Among them, C_0 (mg/L) represents the initial concentration of the binary mixed
160 solution; C_e (mg/L) represents the equilibrium concentration of the binary mixed
161 solution; V (mL) is the volume of the binary mixture, and W (mg) is the mass of the
162 adsorbent.

163 2.6 Adsorption kinetics

164 Taking the binary mixed solution with NH_4^+-N and TP concentration of 350 mg/L.
165 Firstly, pH was adjusted to 7.0, and then 10 mL of the solution was taken and 10 mg of
166 tannic acid modified La-Zn(4,4'-dipy)$(OAc)_2$/BC composite membrane was immersed
167 in it. The concentrations of ammonia nitrogen and total phosphorus at 5, 10, 30, 60, 120,
168 180, 240, 360, 420, 540, 600 and 660 min were measured at 25 ºC.

169 2.7 Adsorption isotherm

170 A binary mixture of NH_4^+-N and TP solution, NH_4^+-N and TP solution were
171 prepared with concentrations of 10, 50, 100, 150, 250, 350, 500, 800 and 1000 mg/L,
172 respectively. Then 10 mg of tannin-modified La-Zn(4,4'-dipy)$(OAc)_2$/BC composite
173 membrane was added to the solution, and oscillation under 25 ºC for 24 hours. The
174 concentrations of ammonia nitrogen and total phosphorus in water were measured by
175 nessler reagent colorimetry and ammonium molybdate spectrophotometry.

176 2.8 Dynamic adsorption

177 A binary mixed solution of NH_4^+-N and TP with a concentration of 50 mg/L was
178 prepared, and pass the water sample at a flow rate of 0.0062 L/min through the
179 composite membrane with a diameter of 3 cm. The concentrations of ammonia nitrogen
180 and total phosphorus in the solution were determined at an interval of 1 hour.

181 # 3. Results and discussion

182 3.1 Characterization results and analysis

183 The crystal structures of Zn(4,4'-dipy)$(OAc)_2$ and La-Zn(4,4'-dipy)$(OAc)_2$ can be
184 determined by X-ray diffraction (XRD). As shown in Figure 2, Zn(4,4'-dipy)$(OAc)_2$
185 showed a higher peak intensity at 2θ=6°, where the peak intensity belongs to Zn^{2+}, the
186 peak strength of La- Zn(4,4'-dipy)$(OAc)_2$ after modification of lanthanum was
187 significantly reduced at 2θ=6°, and a new characteristic peak appeared between
188 2θ=30°-40 °, all of which can account for the payload of lanthanum. This is consistent
189 with the previous research results of our group work. (Wei et al. 2020a)

By scanning electron microscopy (SEM), microstructure of the BC membrane surface show a three-dimensional network cross-linked structure (Figure 3a), which is the special structure of bacterial cellulose. Figure 3b show the load of La-Zn (4,4'-dipy)$(OAc)_2$ was observed on the membrane surface, which confirmed that La-Zn (4,4'-dipy)$(OAc)_2$ and BC could be effectively prepared by tannic acid modified. It is also proved that the addition of La-Zn (4,4'-dipy)$(OAc)_2$ has no effect on the structure of BC.

The FT-IR chart can clearly understand the functional group properties of Zn(4,4'-dipy)$(OAc)_2$ and La-Zn(4,4'-dipy)$(OAc)_2$. As shown in Figure 4, a wide and strong characteristic peak of $-NH_2$ appeared near 3430 cm^{-1}, which is belong to the characteristic peak of an organic ligand named as 4,4'-bipyridine in the Zn(4,4'-dipy)$(OAc)_2$ material. After the intercalation of the lanthanum, the peak strength of the material at 1360 cm^{-1} was enhanced, and the special vibration of nitrate anion appeared at 1560 cm^{-1}, indicating the effective encapsulation of the element La. La-Zn(4,4'-dipy)$(OAc)_2$/BC also showed the characteristic peaks near 1560 cm^{-1} and 1360 cm^{-1}, indicating that La-Zn(4,4'-dipy)$(OAc)_2$ successfully combined with tannin-modified BC.

The TG/DTG of Zn(4,4'-dipy)$(OAc)_2$ and La-Zn(4,4'-dipy)$(OAc)_2$ are shown in Figure 5. It can be seen in the figure that when lanthanum is intercalated in the MOFs material, its mass loss is 20% higher than that of Zn(4,4'-dipy)$(OAc)_2$. The doping of lanthanum element increased the thermal stability of the MOFs. Figure 5(a) showed

211 that the decomposition of the MOFs material can be divided into three stages. The first
212 stage is that when the temperature increases to 100 ºC, Zn(4,4'-dipy)$(OAc)_2$ began to
213 decompose, at this time the mass is reduced by about 6%. The second stage is at 112-
214 187 ºC, the mass is reduced by about 16%, and final stage is at 187-302 ºC, its
215 decomposition rate is significantly lower than the former two stages, the mass has lost
216 about 14%. It can be seen from Figure 5(b) that the decomposition process of La-
217 Zn(4,4'-dipy)$(OAc)_2$ at a heating rate of 10 ºC /min is also divided into three stages,
218 namely 48-155 ºC, 155-237 ºC and 237-508 ºC, with corresponding mass loss of 6%,
219 11% and 7%.

220 3.2 Effect of pH on adsorption

221 The effects of different pH values on the adsorption of ammonia nitrogen and total
222 phosphorus by the composite membrane were compared. As shown in Figure 6, when
223 the pH value of the binary mixed solution is acidic, the adsorption capacity of the
224 composite membrane material for NH_4^+-N in the water should be less than 10 mg/g,
225 which is because the ammonia nitrogen in the water is mainly in form of NH_4^+, and the
226 low pH conditions are not conducive to the adsorption. However, under acidic pH
227 conditions, the adsorption capacity of the composite membrane for total phosphorus is
228 much higher than that of ammonia nitrogen in the water. With the increase of pH value
229 to 7.0, the adsorption capacity of tannic acid modified La-Zn(4,4'-dipy)$(OAc)_2$/BC
230 composite membrane to NH_4^+-N and TP in the water reached the highest. The pH of the
231 solution was adjusted to alkaline, with the increase of OH^-, the competitive adsorption

232 between OH^- and PO_4^{3-} leads to a decrease in the adsorption capacity of the composite
233 membrane to the TP in the binary mixed solution. At this point, the NH_4^+ in the solution
234 rapidly decreases, most of the molecular forms in the water are mainly NH_3, which is
235 not conducive to the adsorption of ammonia nitrogen in the composite membrane.
236 Based on the above trends, the following adsorption experiment was conducted at pH
237 = 7.0.

238 3.3 Adsorption dynamics

239 Q_t is given by formula (2):(Zhang et al. 2020b)

240 $$Q_t=\frac{(C_0-C_t)\times V}{W} \quad (2)$$

241 Among them, Q_t (mg/g) represents the adsorption amount of ammonia nitrogen
242 and total phosphorus at time t, while C_t (mg/L) represents the adsorption equilibrium
243 concentration at time t.

244 Figure 7 showed the kinetics fitting model of tannic acid modified La-Zn(4,4'-
245 dipy)$(OAc)_2$/BC composite membrane adsorption ammonia nitrogen and total
246 phosphorus, within the first 120 min the adsorption capacity of NH_4^+-N and TP in the
247 composite membrane rapidly increased to 133.83 mg/g and 126.08 mg/g. From 120 min
248 to 360 min, the adsorption capacity of NH_4^+-N and TP by the composite membrane
249 increased gradually, The adsorption process reached adsorption equilibrium at 360 min,
250 and the adsorption capacity of the La-Zn(4,4'-dipy)$(OAc)_2$/BC composite membrane
251 gradually saturated. Figure 7 showed that at the beginning of adsorption, the adsorption
252 capacity of NH_4^+-N and TP is almost the same. With the increase of adsorption time, the

adsorption capacity of the adsorbent for NH_4^+-N in the water is higher than its adsorption capacity for the TP. The adsorption data were fitted into quasi-first-order kinetic equations (3) and quasi-second-order kinetic equations (4).(Meng et al. 2019)

$$\ln(Q_e-Q_t)=\ln Q_e-k_1 t \quad (3)$$

$$1/(Q_e-Q_t)=1/Q_e+k_2 t \quad (4)$$

Where, k_1 and k_2 respectively represent the adsorption rate constants of tannic acid modified La-Zn(4,4'-dipy)$(OAc)_2$/BC composite membrane. In addition, the formula (5) is the initial adsorption rate h (mg/(g•min)) of the material, and the half equilibrium time $t_{1/2}$ (min) can be calculated by formula (6).(Li et al. 2019b)

$$h=k_2 Q_e^2 \quad (5)$$

$$t_{1/2}=1/k_2 Q_e \quad (6)$$

According to the data in Table 1, the first order kinetic model was used to fit the adsorption process, and it was found that the coefficient of determination values (R^2) of the composite membrane adsorption were 0.97844 and 0.97604, less than the values of R^2 of the second order kinetic equation were 0.99097 and 0.98992. The adsorption process of the composite membrane was in accordance with quasi second order kinetic equation. The adsorption capacities of the NH_4^+-N and TP calculated by the formula was 193.52 mg/g and 162.58 mg/g, respectively. The adsorption rate constants of the composite membrane are 0.00010242 g/mg/min and 0.00018993 g/mg/min, respectively. The fitting results prove that the adsorption process is mainly chemical adsorption.

274 3.4 Adsorption isotherm

275 The adsorption effect of tannic acid modified La-Zn(4,4'-dipy)$(OAc)_2$/BC
276 composite membrane on ammonia nitrogen and total phosphorus in binary mixed
277 solution was studied by static adsorption experiment. Use the following equations (7)
278 and (8) to fit the data to the Langmuir and Freundlich equations:(Xu et al. 2018; Zheng
279 et al. 2019; Zheng et al. 2020; Zhuo et al. 2018)

280 $$Q_e=\frac{K_L Q_m C_e}{1+K_L C_e} \quad (7)$$

281 $$Q_e=K_F C_e^{1/n} \quad (8)$$

282 Q_m (mg/L) in formula (7) represents the maximum adsorbent adsorption capacity,
283 while K_L (L/mg) refers to Langmuir binding constant, which depends on temperature
284 and adsorption heat. In formula (8), 1/n represents the Freundlich constant, which
285 depends on the adsorption system. K_F (mg/g) is a constant, depending on the
286 characteristics and quantity of the adsorbed material.

287 The advantages of adsorption can be determined by calculating the separation
288 factor R_L, whose formula is as follows(9):(Basnett et al. 2012; Xu et al. 2020; Zhang et
289 al. 2020b)

290 $$R_L=\frac{1}{1+C_m K_L} \quad (9)$$

291 Figure 8 compares the adsorption capacity of tannic acid modified La-Zn(4,4'-
292 dipy)$(OAc)_2$/BC composite membrane to ammonia nitrogen and total phosphorus.
293 Figure 8 shows that the adsorption effect of tannic acid modified La-Zn(4,4'-
294 dipy)$(OAc)_2$/BC composite membrane on ammonia nitrogen is better than that on total

295 phosphorus. According to the data in Table 2, the saturated adsorption capacity of NH_4^+-
296 N in the binary mixed solution is 466.33 mg/g, while the saturated adsorption capacity
297 Q_m of single-component NH_4^+-N is 482.35 mg/g. The saturated adsorption capacity of
298 total phosphorus in the binary mixed solution was 370.94 mg/g, while the saturated
299 adsorption capacity of single component total phosphorus was 374.71 mg/g, which also
300 showed a decrease in adsorption capacity, but with a small decrease. Our previous
301 studies have found that La-modified MOFs has a selective adsorption and separation
302 effect on total phosphorus(Wei et al. 2020b), but tannic acid has no selective adsorption
303 effect on both total phosphorus and ammonia nitrogen, which can explain why the effect
304 of the tannic acid modified La-Zn(4,4'-dipy)$(OAc)_2$/BC composite membrane on
305 phosphorus decreased less than that of ammonia nitrogen.

306 According to the fitting data of the Langmuir and Freundlich equations in Table 2
307 and Table 3, Langmuir fitting equation R^2 is greater than the Freundlich fitting equation.
308 Therefore, it can be proved that the adsorption of ammonia nitrogen and total
309 phosphorus by tannic acid modified La-Zn(4,4'-dipy)$(OAc)_2$/BC composite membrane
310 is more likely to conform to the Langmuir equation, indicating that it is a monolayer
311 adsorption process. In addition, R_L is greater than 0 and less than 1, indicating that the
312 adsorption process of NH_4^+-N and TP by the composite membrane was the preferred
313 adsorption process.

314 3.5 Dynamic adsorption

315 Dynamic adsorption experiments were carried out on the binary mixed solution of

316 ammonia nitrogen and total phosphorus. Figure 9 showed the penetration curves of
317 ammonia nitrogen and total phosphorus in the mixed solution adsorbed by the
318 composite membrane. Penetration curve is generally an S-shaped curve, and the
319 inclination of the S-shaped curve is different under different circumstances. The
320 penetration point can only be accurately obtained through experiments. Take the point
321 in the figure where the adsorption capacity rises sharply as the penetration point. The
322 adsorption of NH_4^+-N and TP by the tannic acid modified La-Zn(4,4'-dipy)$(OAc)_2$/BC
323 composite membrane showed a penetration point between 60 and 120 min. The end
324 point of the penetration curve was taken as the inflexion point at the top of the S-shaped
325 curve close to the initial concentration. Therefore, the penetration curve reached the end
326 point at 480 min, and the penetration time of the composite membrane for NH_4^+-N and
327 TP in the water was 8 hours at the initial concentration of 50 mg/L and a flow rate of
328 0.0062 L/min.

329 3.6 Reusability tests

330 The amount of adsorbent used greatly affects the cost of treating sewage, so it is
331 very important to improve the reusability of adsorbent and minimize the amount of
332 adsorbent required. The adsorbed tannin-modified La-Zn(4,4'-dipy)$(OAc)_2$/BC
333 composite membrane was transferred to the eluent (10% glacial acetic acid) for 48
334 hours and rinsed with ultra-pure water for three times before drying. The whole
335 adsorption desorption process was repeated 5 times. As can be seen from Figure 10,
336 after 5 cycles, the adsorption capacity of ammonia nitrogen of the composite membrane

decreased to 80.94%, and the adsorption capacity of total phosphorus decreased to 82.91%, which we believe was mainly caused by eluting the imprinted binding site. Although the adsorption capacity of the composite membrane decreased after 5 cycles, it still remained above 80% with good reusability and could be used as a reliable adsorbent for the separation of ammonia nitrogen and total phosphorus in water.

4. Conclusions

In this experiment, the tannic acid modified La-Zn(4,4'-dipy)$(OAc)_2$/BC composite membrane was prepared for adsorption of total phosphorus and ammonia nitrogen. When the pH is 7.0, the adsorption capacity of the composite membrane material to the binary mixed solution of ammonia nitrogen and total phosphorus in water were 466.33 mg/g and 370.94 mg/g. The data fitting of total phosphorus and ammonia nitrogen in the water adsorbed by the tannic acid modified La-Zn(4,4'-dipy)$(OAc)_2$/BC composite membrane conformed to the Langmuir equation and the quasi second order kinetic equation, which showed that the adsorption reaction belongs to monolayer chemical adsorption. The equilibrium between the La-Zn(4,4'-dipy)$(OAc)_2$/BC composite membrane and the water sample can be obtained by the dynamic adsorption breakthrough curve. All these results indicate the tannic acid modified La-Zn(4,4'-dipy)$(OAc)_2$/BC composite membrane has good adsorption properties for ammonia nitrogen and total phosphorus, and can effectively adsorb pollutants in water.

5. Declarations

5.1 Ethics approval and consent to participate

Not applicable.

5.2 Consent for publication

Not applicable.

5.3 Availability of data and materials

All data generated or analysed during this study are included in this published article.

5.4 Competing interests

The authors declare that they have no competing interests" in this section.

5.5 Acknowledgements

The authors thank the National Natural Science Foundation of China (Grant Nos. 21876015, 21808018), Applied Basic Research of Changzhou (Grant No. CJ20180055), Natural Science Research of Jiangsu Higher Education Institutions of China (Grant No. 18KJB610002), Science and Technology Support Program of Changzhou (Grant No. CE20185015). The authors are grateful to Wang Liang from Shiyanjia Laboratory for providing us with XPS analysis.

5.6 Authors' contributions

ZXD was the main contributor to the manuscript, and SW was used to analyze and interpret the data of material properties. WN, LLL, BTT and ZY were used to prepare the composite membrane, while ZYZ, LZY, and OHX proofread and checked the article. All the authors have seen the manuscript and approved to submit to your journal.

References

Basnett P, Knowles JC, Pishbin F, Smith C, Keshavarz T, Boccaccini AR, Roy I (2012) Novel Biodegradable and Biocompatible Poly(3-hydroxyoctanoate)/Bacterial Cellulose Composites Advanced Engineering Materials 14:B330-B343 doi:10.1002/adem.201180076

Bormans M, Maršálek B, Jančula D (2016) Controlling internal phosphorus loading in lakes by physical methods to reduce cyanobacterial blooms: a review Aquat Ecol 50:407-422 doi:10.1007/s10452-015-9564-x

Copetti D et al. (2016) Eutrophication management in surface waters using lanthanum modified bentonite: A review Water Res 97:162-174 doi:10.1016/j.watres.2015.11.056

Ejima H et al. (2013) One-Step Assembly of Coordination Complexes for Versatile Film and Particle Engineering Science (New York, NY) 341:154-157 doi:10.1126/science.1237265

Li A, Strokal M, Bai Z, Kroeze C, Ma L (2019a) How to avoid coastal eutrophication - a back-casting study for the North China Plain Sci Total Environ 692:676-690 doi:https://doi.org/10.1016/j.scitotenv.2019.07.306

Li Q et al. (2020) Tannic acid assisted interfacial polymerization based loose thin-film composite NF membrane for dye/salt separation Desalination 479:114343

Li S et al. (2019b) Graphene oxide based dopamine mussel-like cross-linked polyethylene imine nanocomposite coating with enhanced hexavalent uranium

adsorption Journal of Materials Chemistry A 7:16902-16911 doi:10.1039/c9ta04562g

Meng K et al. (2019) Efficient Adsorption of the Cd(II) and As(V) Using Novel Adsorbent Ferrihydrite/Manganese Dioxide Composites ACS Omega 4:18627-18636 doi:10.1021/acsomega.9b02431

Qiu H, Ye M, Zeng Q, Li W, Fortner J, Liu L, Yang L (2019) Fabrication of agricultural waste supported UiO-66 nanoparticles with high utilization in phosphate removal from water Chem Eng J 360:621-630 doi:https://doi.org/10.1016/j.cej.2018.12.017

Schindler DW (2012) The dilemma of controlling cultural eutrophication of lakes Proc R Soc B 279:4322-4333 doi:10.1098/rspb.2012.1032

Shi K, Zhang Y, Zhang Y, Li N, Qin B, Zhu G, Zhou Y (2019) Phenology of Phytoplankton Blooms in a Trophic Lake Observed from Long-Term MODIS Data Environ Sci Technol 53:2324-2331 doi:10.1021/acs.est.8b06887

Shi M et al. (2020) Combining tannic acid-modified support and a green co-solvent for high performance reverse osmosis membranes J Membr Sci 595:117474

Taipale SJ, Vuorio K, Aalto SL, Peltomaa E, Tiirola M (2019) Eutrophication reduces the nutritional value of phytoplankton in boreal lakes Environ Res 179:108836 doi:https://doi.org/10.1016/j.envres.2019.108836

Wang J, Cahyadi A, Wu B, Pee W, Fane AG, Chew JW (2020) The roles of particles in enhancing membrane filtration: A review J Membr Sci 595:117570

421 Wei N, Zheng X, Li Q, Gong C, Ou H, Li Z (2020a) Construction of lanthanum
422 modified MOFs graphene oxide composite membrane for high selective
423 phosphorus recovery and water purification J Colloid Interface Sci 565:337-344
424 doi:https://doi.org/10.1016/j.jcis.2020.01.031
425 Wei N, Zheng X, Li Q, Gong C, Ou H, Li Z (2020b) Construction of lanthanum
426 modified MOFs graphene oxide composite membrane for high selective
427 phosphorus recovery and water purification J Colloid Interface Sci 565:337-344
428 doi:10.1016/j.jcis.2020.01.031
429 Xu X et al. (2020) Film-like bacterial cellulose based molecularly imprinted materials
430 for highly efficient recognition and adsorption of cresol isomers Chem Eng J
431 382 doi:10.1016/j.cej.2019.123007
432 Xu Y-T, Dai Y, Nguyen T-D, Hamad WY, MacLachlan MJ (2018) Aerogel materials
433 with periodic structures imprinted with cellulose nanocrystals Nanoscale
434 10:3805-3812 doi:10.1039/c7nr07719j
435 Yan K et al. (2019) Phosphorus mitigation remains critical in water protection: A review
436 and meta-analysis from one of China's most eutrophicated lakes Sci Total
437 Environ 689:1336-1347 doi:10.1016/j.scitotenv.2019.06.302
438 Zhang J, Wang C, Jiang X, Song Z, Xie Z (2020a) Effects of human-induced
439 eutrophication on macroinvertebrate spatiotemporal dynamics in Lake Dianchi,
440 a large shallow plateau lake in China Environ Sci Pollut Res 27:13066-13080
441 doi:10.1007/s11356-020-07773-w

442 Zhang X, Li B, Xu H, Wells M, Tefsen B, Qin B (2019) Effect of micronutrients on
443 algae in different regions of Taihu, a large, spatially diverse, hypereutrophic lake
444 Water Res 151:500-514
445 Zhang Y, Zheng X, Bian T, Zhang Y, Mei J, Li Z (2020b) Phosphorylated-
446 CNC/MWCNT thin films-toward efficient adsorption of rare earth La(III)
447 Cellulose 27:3379-3390 doi:10.1007/s10570-020-03012-0
448 Zhao R, Li X, Sun B, Li Y, Li Y, Yang R, Wang C (2017) Branched polyethylenimine
449 grafted electrospun polyacrylonitrile fiber membrane: a novel and effective
450 adsorbent for Cr(VI) remediation in wastewater J Mater Chem 5:1133-1144
451 Zheng X, Zhang Y, Bian T, Wang D, Li Z (2019) One-step fabrication of imprinted
452 mesoporous cellulose nanocrystals films for selective separation and recovery
453 of Nd(III) Cellulose 26:5571-5582 doi:10.1007/s10570-019-02482-1
454 Zheng XD, Zhang Y, Bian TT, Zhang YZ, Li ZY, Pan JM (2020) Oxidized carbon
455 materials cooperative construct ionic imprinted cellulose nanocrystals films for
456 efficient adsorption of Dy(III) Chem Eng J 381:10
457 doi:10.1016/j.cej.2019.122669
458 Zhu Z et al. (2017) Ultrahigh adsorption capacity of anionic dyes with sharp selectivity
459 through the cationic charged hybrid nanofibrous membranes Chem Eng J
460 313:957-966
461 Zhuo H et al. (2018) A Supercompressible, Elastic, and Bendable Carbon Aerogel with
462 Ultrasensitive Detection Limits for Compression Strain, Pressure, and Bending

Angle Advanced Materials 30 doi:10.1002/adma.201706705

Table and Figure Captions

Table 1 Kinetic fitting results of composite membrane adsorbing binary component solution in water

Table 2 Single-component adsorption Langmuir and Freundlich equation fitting results

Table 3 Fitting results of Langmuir and Freundlich equation for binary component adsorption

Figure 1 Synthesis of tannic acid modified La Zn(4,4'-dipy)$(OAc)_2$/BC composite membrane

Figure 2 XRD patterns of Zn(4,4’-dipy)$(OAc)_2$ and La-Zn(4,4’-dipy)$(OAc)_2$

Figure 3 SEM images of two films: (a) BC, (b) La-Zn(4,4'-dipy)$(OAc)_2$/BC

Figure 4 FT-IR comparison of BC, Zn(4,4’-dipy)$(OAc)_2$, La-Zn(4,4’-dipy)$(OAc)_2$ and La-Zn(4,4’-dipy)$(OAc)_2$/BC

Figure 5 TG/DTG diagram of Zn(4,4’-dipy)$(OAc)_2$ and La-Zn(4,4’-dipy)$(OAc)_2$ (a is Zn(4,4’-dipy)$(OAc)_2$ TG/DTG diagram; b is La-Zn(4,4’-dipy)$(OAc)_2$ TG/DTG diagram)

Figure 6 Effect of pH on the adsorption of binary mixed solution of ammonia nitrogen and total phosphorus by the composite membrane

Figure 7 Comparison of kinetic adsorption of ammonia nitrogen and total phosphorus in binary mixed solution

Figure 8 Adsorption isotherm of ammonia nitrogen and total phosphorus (a is single-component adsorption, b is the competitive adsorption)

Figure 9 Dynamic adsorption comparisons of ammonia nitrogen and total phosphorus in binary mixed solution (a is the penetration curve of ammonia nitrogen adsorption, b is the penetration curve of total phosphorus adsorption)

Figure 10 Adsorption capacity of composite membrane over 5 cycles

Figures

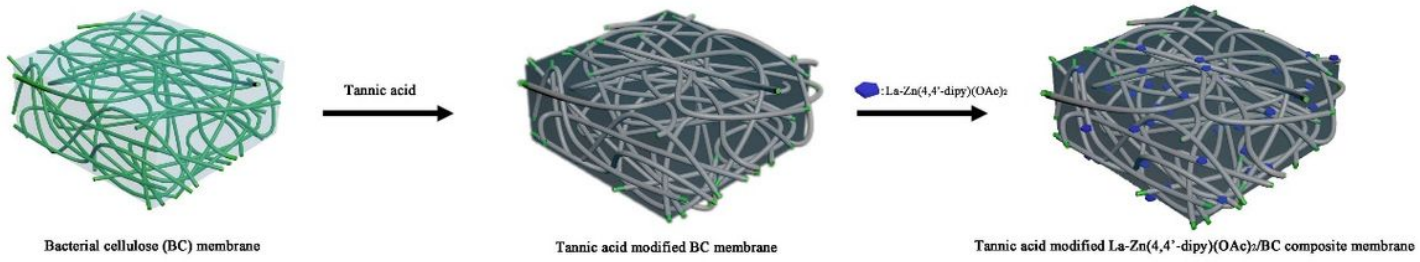

Figure 1

Synthesis of tannic acid modified La Zn(4,4'-dipy)(OAc)2/BC composite membrane

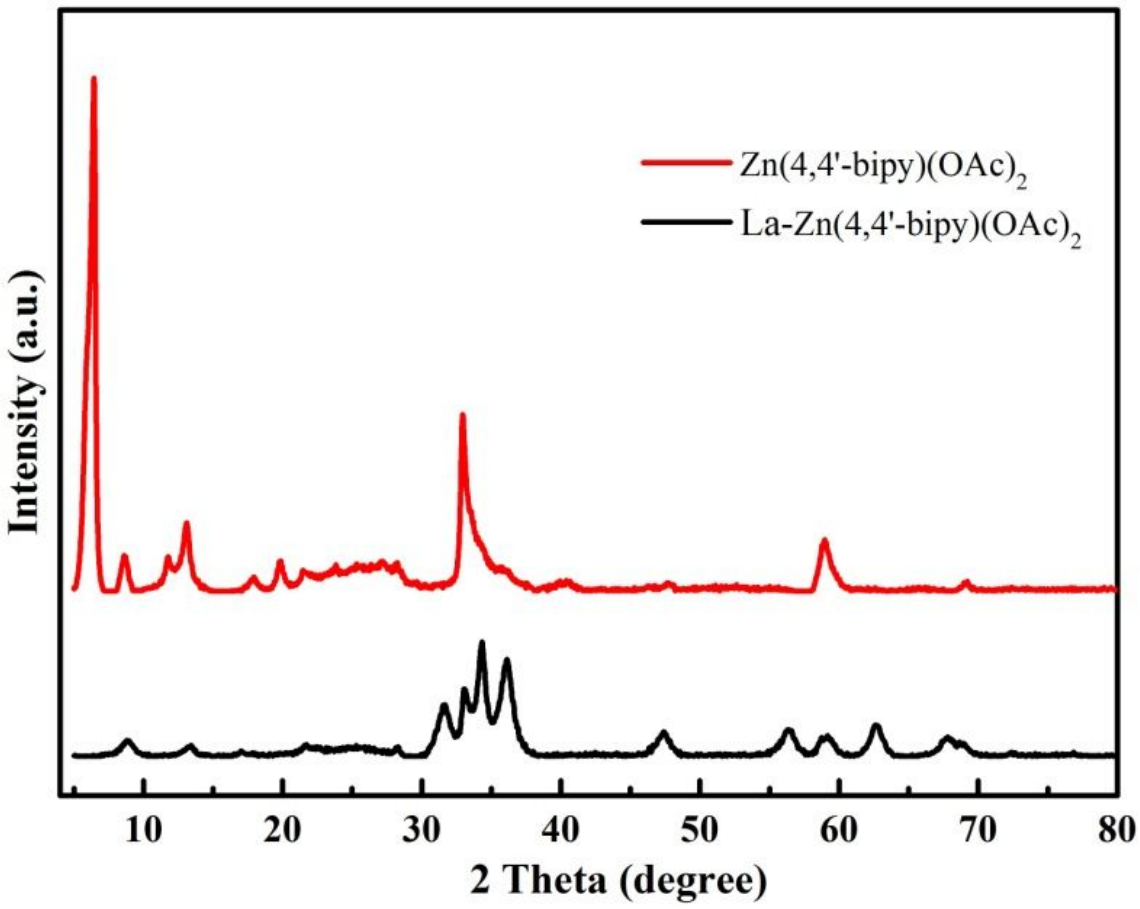

Figure 2

XRD patterns of Zn(4,4’-dipy)(OAc)2 and La-Zn(4,4’-dipy)(OAc)2

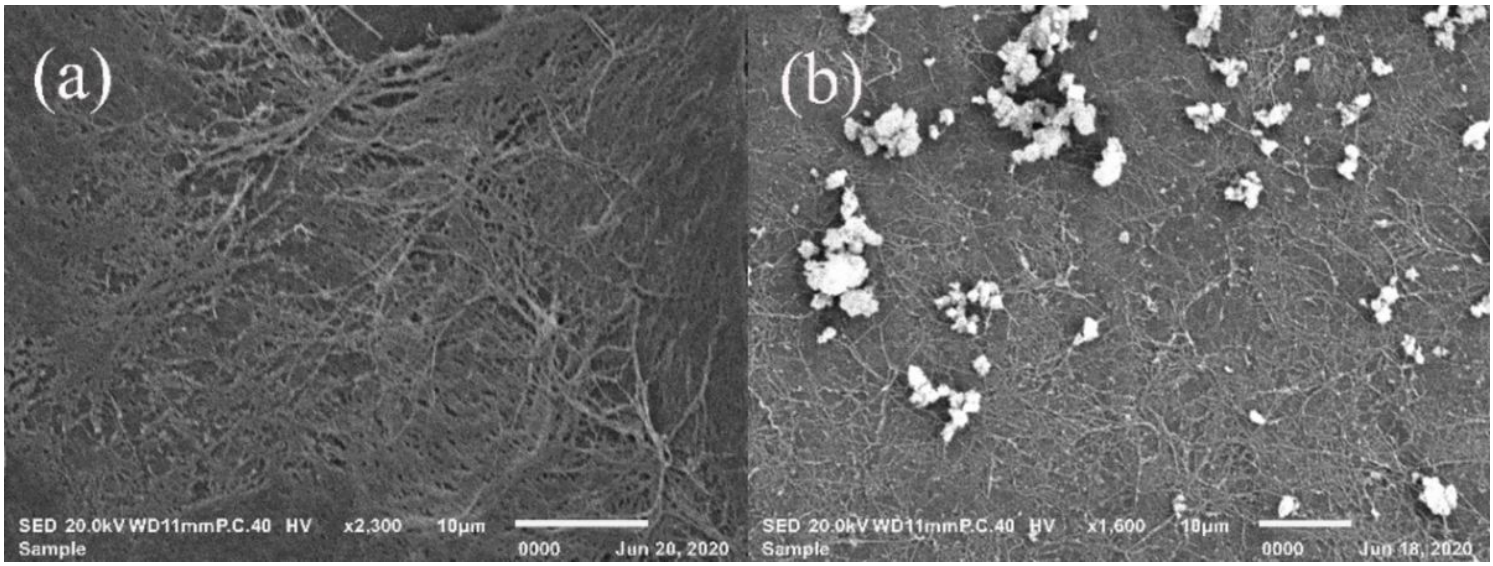

Figure 3

SEM images of two films: (a) BC, (b) La-Zn(4,4'-dipy)(OAc)2/BC

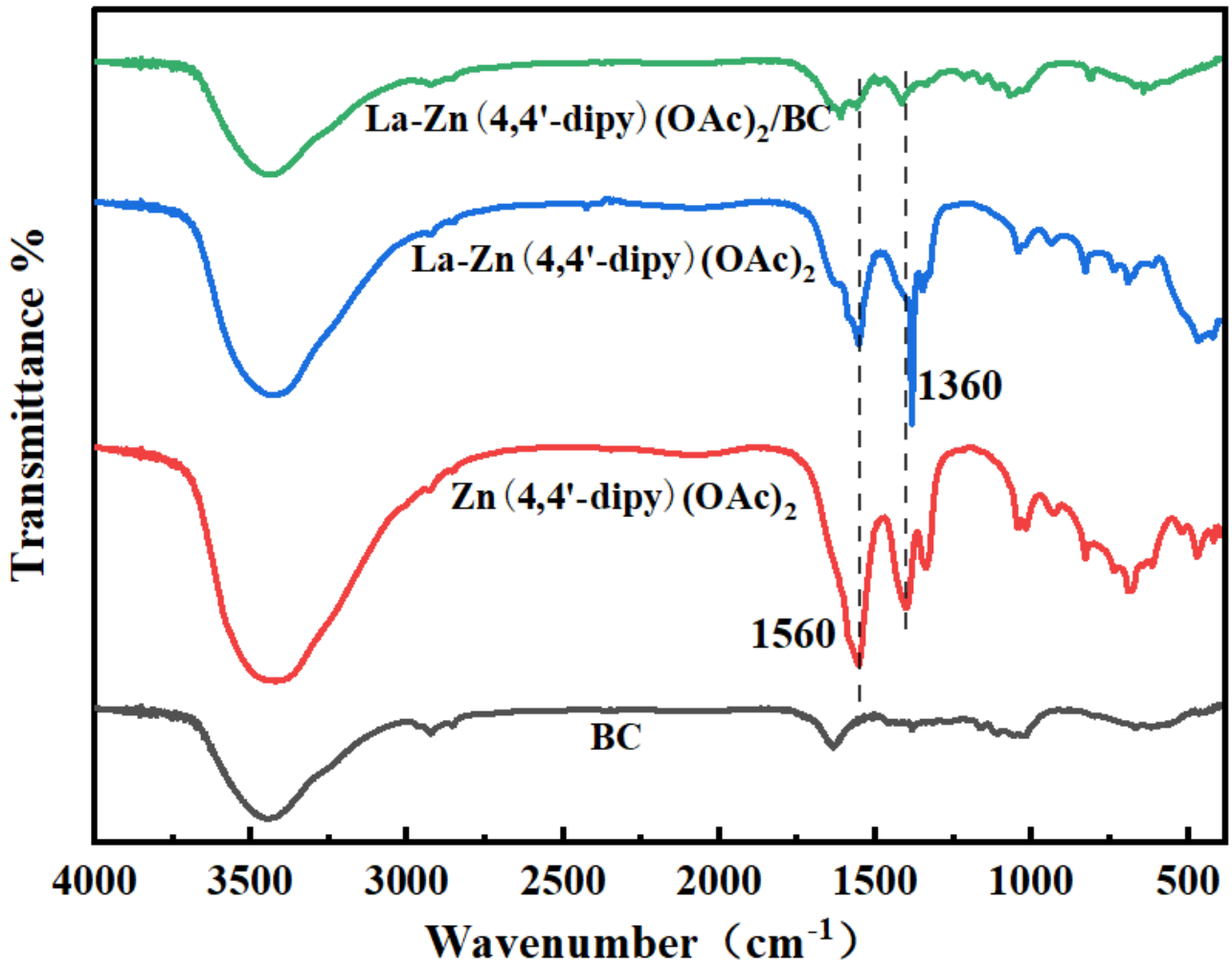

Figure 4

FT-IR comparison of BC, Zn(4,4’-dipy)(OAc)2, La-Zn(4,4’-dipy)(OAc)2 and La-Zn(4,4’-dipy)(OAc)2/BC

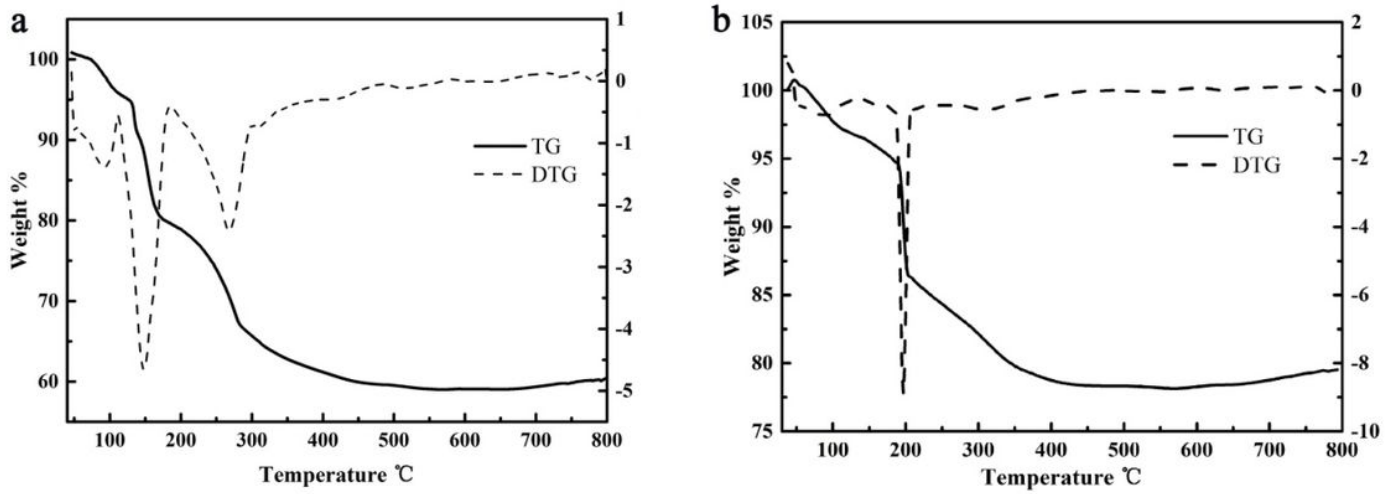

Figure 5

TG/DTG diagram of Zn(4,4’-dipy)(OAc)2 and La-Zn(4,4’-dipy)(OAc)2 (a is Zn(4,4’-dipy)(OAc)2 TG/DTG diagram; b is La-Zn(4,4’-dipy)(OAc)2 TG/DTG diagram)

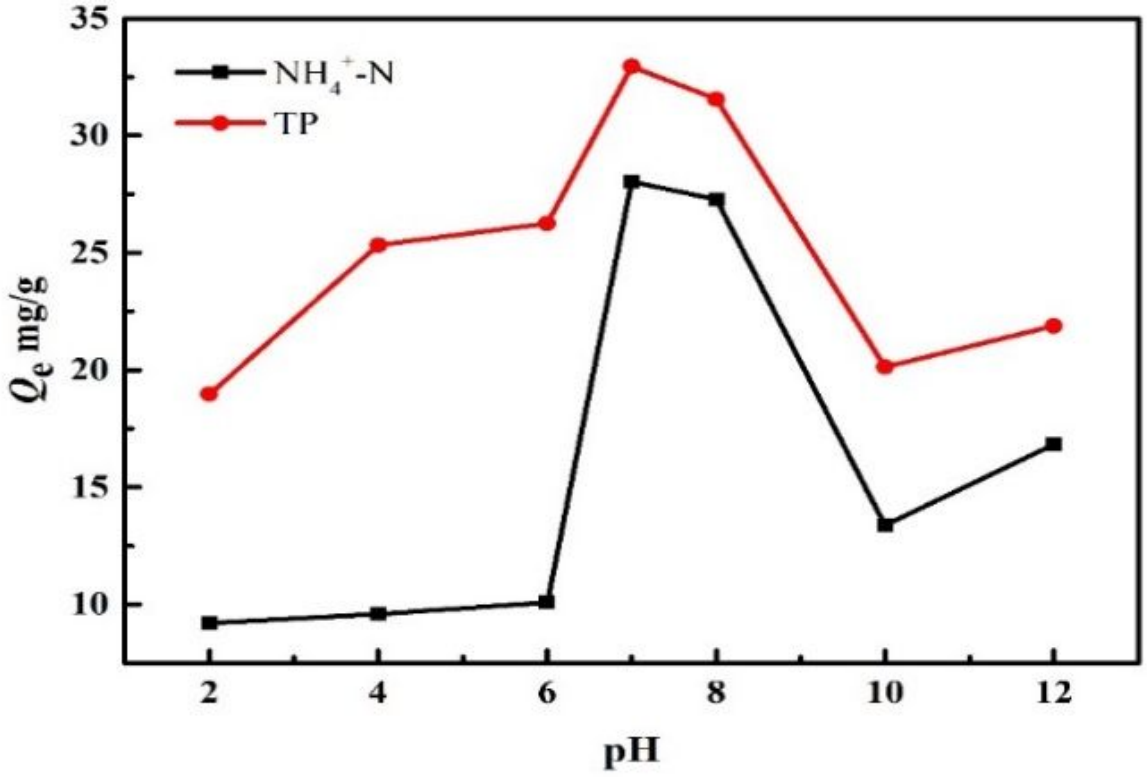

Figure 6

Effect of pH on the adsorption of binary mixed solution of ammonia nitrogen and total phosphorus by the composite membrane

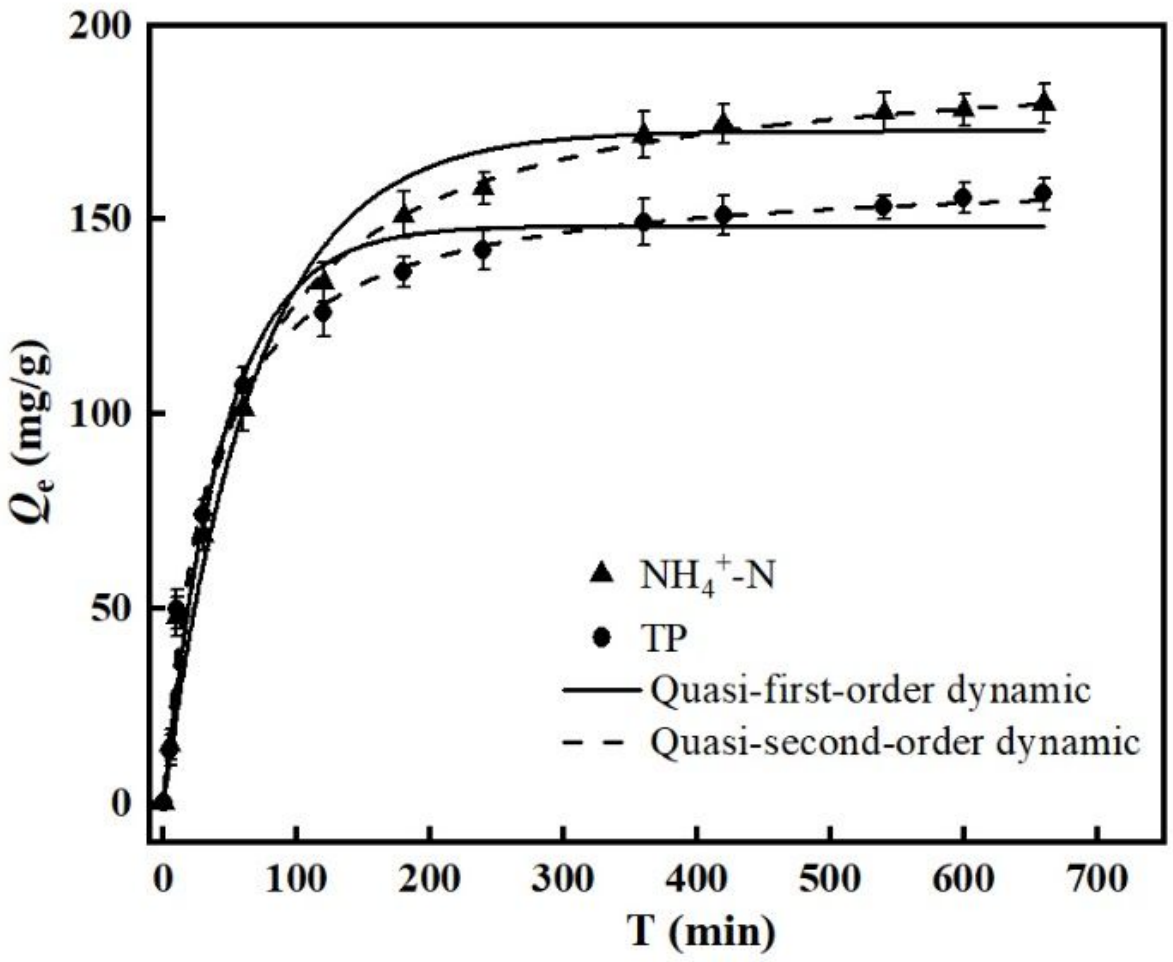

Figure 7

Comparison of kinetic adsorption of ammonia nitrogen and total phosphorus in binary mixed solution

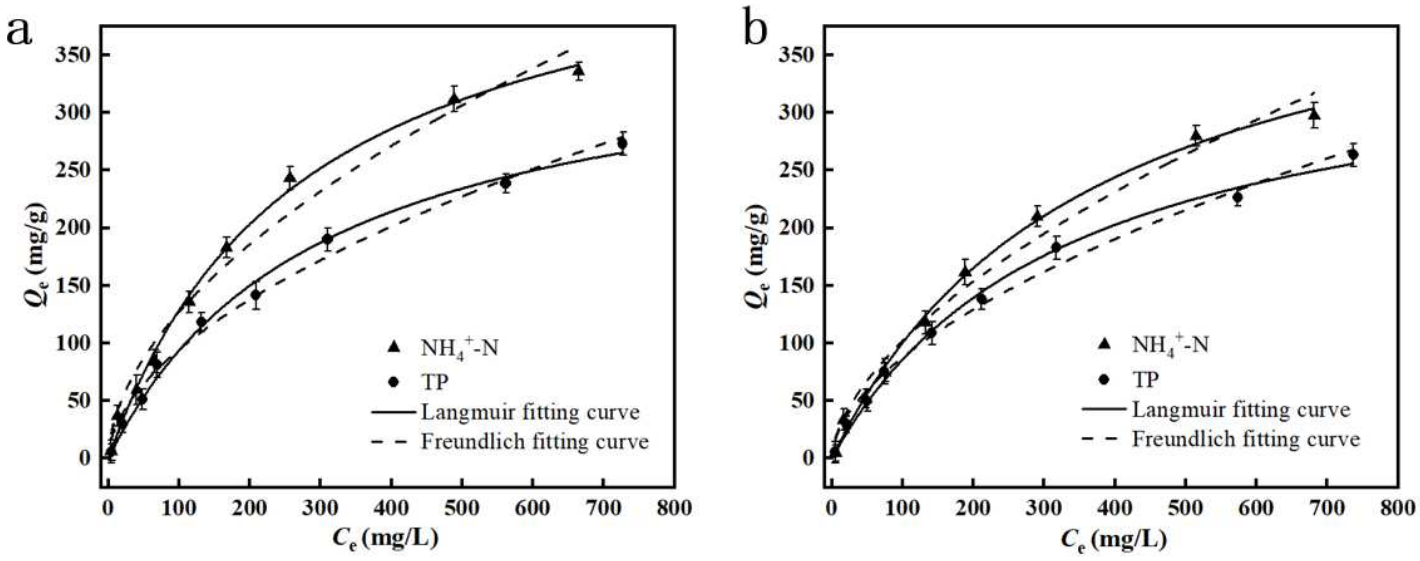

Figure 8

Adsorption isotherm of ammonia nitrogen and total phosphorus (a is single-component adsorption, b is the competitive adsorption)

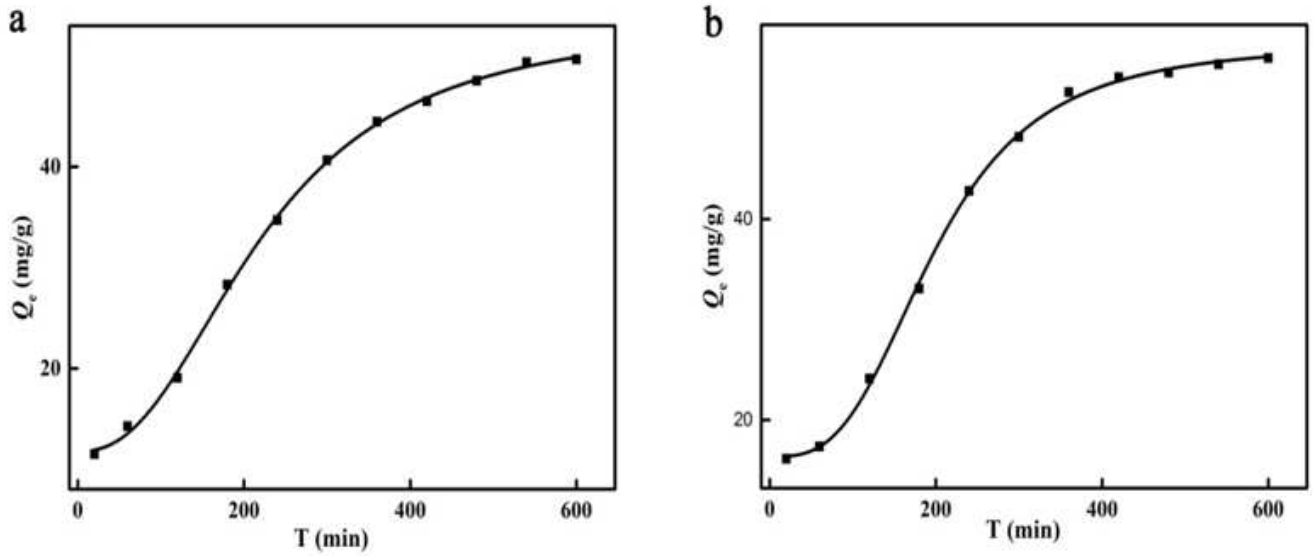

Figure 9

Dynamic adsorption comparisons of ammonia nitrogen and total phosphorus in binary mixed solution (a is the penetration curve of ammonia nitrogen adsorption, b is the penetration curve of total phosphorus adsorption)

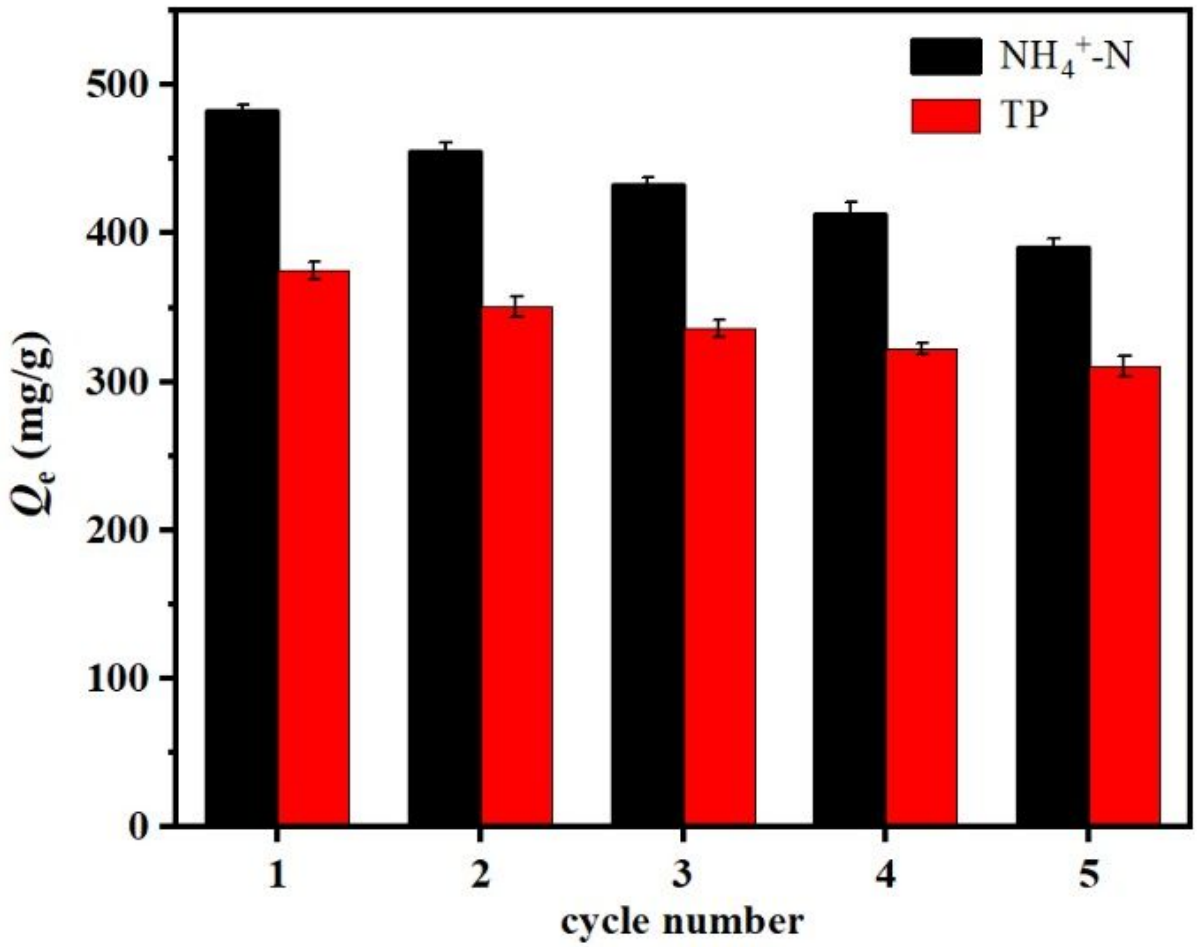

Figure 10

Adsorption capacity of composite membrane over 5 cycles